Coastal Dynamics 2017
Paper No. 261

DRIVERS OF CHANNEL-SHOAL MORPHODYNAMICS AT THE OUTER WESER ESTUARY

Gerald Herrling[1], Markus Benninghoff[1], Anna Zorndt[2] and Christian Winter[1]

Abstract

Morphodynamics of channel-shoal and intertidal flat systems, as the Outer Weser estuary in the southern German Wadden Sea, are driven by the hydrodynamic forcing of tides, wind and waves. The latter can be differentiated into locally generated wind waves and offshore sea state. Wave forcing of intertidal environments has often been neglected in related morphodynamic modelling studies due to its complexity and the associated computational effort of two-way coupling between waves and currents. In this study, we reflect on the relative importance of each hydrodynamic driver estimated and quantified based on their individual morphological feedback highlighted for sub- and intertidal environments. We further evaluate channel-shoal morphodynamics in response to fair-weather conditions in comparison to an extreme storm event.

Key words: Wadden Sea, tidal flats, hydrodynamic forcing, scenario simulations, extreme storm, Delft3D

1. Introduction

Morphodynamics of intertidal channel-shoal systems are primarily governed by the interaction of tidal, wave and wind forces (Le Hir et al., 2000). Typical morphological changes comprise tidal channel meandering and/or migration with related shoal erosion or accretion. Intertidal flat systems, e.g. in the Wadden Sea, are likely to response to accelerated sea level rise and to potential changes in storm frequency and direction. An improved knowledge of the system's morphodynamic response to hydrodynamic drivers is essential when aiming the long-term sustainability of the intertidal ecosystem and the preservation of its function as a natural coastal defense.

Given a suitable model realization (configuration) for the domain of investigation, the system's morphological response to distinct drivers which is normally obscured by the non-linear interaction of the natural system may be deciphered by dedicated numerical model experiments (e.g. Elias and Hansen, 2013; Herrling and Winter, 2014). This is done in a step-by-step exclusion of certain underlying physical processes in order to identify (isolate) the system's response to the governing physical mechanisms. The application of process-based models thus implies that reality is reduced in the way that no relevant processes are neglected, but the computational effort is still acceptable. Nowadays, mid- and long-term morphodynamic modelling studies of channel-shoal systems still tend to neglect wave forcing to economize computational time (e.g. Dissanayake et al., 2012; Hofstede et al., 2016).

Recent studies have evaluated the effect of tidal forcing versus wave forcing based on observations and model studies at channel-shoal cross-sections and intertidal flats (e.g. Hu et al., 2015; Hunt et al., 2016; Zhou et al., 2015). Common sense is the formation of a morphological equilibrium where the tidal flats adapt to tide- or wave-dominant forcing conditions with convex-up or concave-up hypsometries, respectively (Friedrichs, 2011; Friedrichs and Aubrey, 1996, 1988). Wave conditions vary in their origin and intensity: Locally-generated fetch-limited wind waves, more energetic sea waves or even remotely-generated swell have to be taken into consideration. It is thus important to investigate larger morphological units and scales to identify the relative importance of wave energy versus tidal forcing at channel-shoal systems. Previous large-scale model studies have used bed shear stresses (Kösters and Winter, 2014) as proxies to estimate the effect of different hydrodynamic drivers on the morphological activity in the German Bight. The authors identified waves to play a significant role on morphodynamic processes in the foreshore area of the Wadden Sea.

[1]MARUM, Centre for Marine Environmental Sciences, University of Bremen, Germany. gherrling@marum.de, mbenninghoff@marum.de, cwinter@marum.de

[2]BAW, Federal Waterways Engineering and Research Institute, Hamburg, Germany. anna.zorndt@baw.de

In this study we evaluate outer estuarine channel-shoal dynamics by combining the analysis of morphological monitoring data with high-resolution morphodynamic modelling. A focus is set on their evolution in reaction to different hydrodynamic forcings like tides, wind-driven currents, waves under fair-weather and high energy storm conditions. As an example the Outer Weser region was chosen, and a tidal channel system serves as a reference site: Availability of almost annual bathymetrical observations of the tidal channel Fedderwarder Priel (FWP) and its morphological development largely independent from maintenance dredging of the main Weser navigational channel make this tributary a suitable study area (Fig. 1). Morphodynamic modelling is applied to interpolate between observations and relate sediment dynamics to different forcing scenarios. Interacting processes are separated in a way that the effect of a particular driver can be evaluated on the basis of morphological responses that are assessed on different spatial scales and for sub- and intertidal areas.

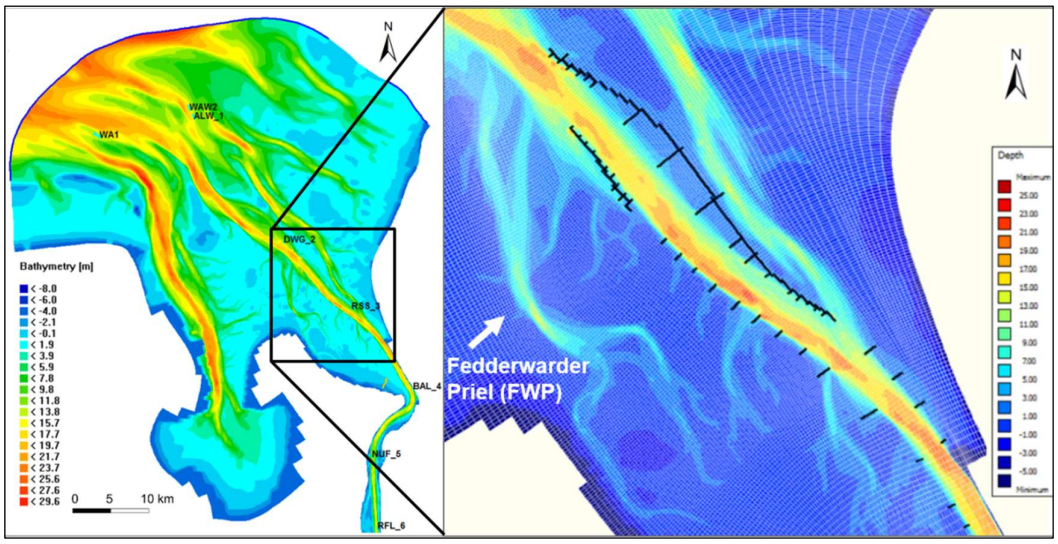

Figure 1. Study area Outer Weser in the German Wadden Sea, southern North Sea; the channel-shoal system 'Fedderwarder Priel' (FWP) is a tributary tidal channel of the Outer Weser estuary.

2. Methodology

2.1. Model system

A hydro-morphodynamic model for the Outer Weser domain has been set-up and applied in a two-dimensional, depth-integrated configuration by applying the process-based modeling system Delft3D (Deltares, 2014). The numerical model solves the shallow water equations and continuity equation on a staggered model grid by use of an implicit finite-difference-scheme. A two-way coupling between the hydrodynamic model (FLOW module) and the spectral wave model SWAN (Booij et al., 1999; Ris et al., 1999) is realized by incorporating the depth-integrated wave forces (i.e. radiation stresses) in the momentum equation of the hydrodynamic module. Instead of using the hydraulic bed roughness coefficient as a calibration (tuning) parameter, a bed roughness predictor (van Rijn, 2007) has been applied. For a detailed description of the equations and implementation into Delft3D, see Lesser et al. (2004) or the documentation distributed with the modeling system (Deltares 2014).

2.2. Model scenarios

Model simulations have been set-up to simulate outer estuarine hydro- and morphodynamics and are driven by real-time boundary conditions of tides, wind, waves and riverine discharge. We differentiate the

morphological feedback in response to average (mostly fair-weather) and severe storm conditions. Simulation periods between June and Nov. 2012 (1) and between Nov. 5th and 11th 2007 (2) represent average hydrodynamics and an extreme storm event. The morphological response to the forcing of each scenario is separated with respect to distinct hydrodynamic drivers. We differentiate in between tides (t), wind shear-stress (w), local fetch-limited wind waves (ww) and offshore sea and swell waves (sw) as observed offshore and imposed as seaward model boundary values. A number of simulations was executed each with a different combination of hydrodynamic boundary conditions, i.e. driving forces. Adequate post-processing methods were applied to separate the net morphological evolution as a result of each simulation into the relative response to each hydrodynamic driver. To segregate the morphological response to sea waves, for example, the morphological state at the end of a simulation driven by tides alone is subtracted from the morphological state simulated by tides and additional sea waves. The observed offshore sea state is imposed at the seaward boundary. The energy distribution of sea waves is computed with respect to their propagation into the model domain. The effect of local wind-induced currents following from wind shear-stress onto the water surface (FLOW module) and/or the effect of locally generated fetch-limited, short wind waves (wave module SWAN) are thus not considered and need to be segregated in a different combination. Net morphological changes with respect to each hydrodynamic driver are integrated and satisfactorily verified against the simulated evolution as response to the drivers interacting altogether. Table 1 gives an overview of the different forcing scenarios considered hereafter.

Table 1. Overview of forcing scenarios

Forcing conditions	Scenario	Drivers	Control area
average hydrodynamic conditions dominated by fair-weather from 01. Jun. to 31.Nov. 2012	1t	tides	Outer Weser from Bremerhaven to widening of main inlet (navigational) channel
	1w	wind stress	
	1ww	wind waves	
	1sw	sea waves	
	1 currents (t & w)	tides + wind stress	tidal basin of the channel Fedderwarder Priel (FWP) with smaller tributaries
	1 waves (ww & sw)	wind waves + sea waves	
extreme storm event 'Tilo' from 05. to 11. Nov. 2007	2 currents (t & w)	tides + wind stress	
	2 waves (ww & sw)	wind waves + sea waves	

2.3. Model set-up

2.3.1. Numerical grids and bathymetry

The model is set-up in a depth-integrated (2DH) configuration. The spatial resolution of the curvilinear grid used in FLOW is 300 to 900 meters at the seaward boundary with maximal resolutions at the main navigational channel; grid lines converge along the main navigational channel to spatial resolutions of 50 to 150 meters at the area of interest between Fedderwarder Priel and Bremerhaven (Fig. 1). Gridlines along the navigational channel and in the Fedderwarder Priel are well aligned with the main current; here, cross-channel resolutions are approx. 40 meters.

The numerical grid being used for wave simulations in SWAN is based on the aforementioned grid at the Outer Weser area (FLOW) but has its landward limit close to Bremerhaven; upstream of Bremerhaven no wave-current interaction is simulated. The seaward boundary of the SWAN grid is aligned parallel to the open sea boundary of the FLOW grid but extends approx. 3 km in seaward direction to the location of the wave buoy “Elbe” where wave measurements are available to be used to force the wave model.

A digital elevation model with overall distances of post-processed point data of 25 meters has been made available by the authorities and covers bathymetrical data surveyed in the years 2011 and 2012. Data has been interpolated onto the abovementioned numerical grids. Data on elevations of training walls and groins are incorporated as structures aligning grid cells. Their effect on the flow at different stages of the tide and flooding heights is parameterized.

For the spatial comparability of data during post-processing procedures the morphological evolution of both scenario simulations need to be comparable at a given horizontal position. At a state chronically halfway between June and Nov. 2012, the morphology and the sediment grain-size distribution of the simulation representing average hydrodynamic conditions is output and used as initial bathymetry and surface

sedimentology set at the beginning of the storm simulation (7 days in Nov. 2007). This ensures morphological states in response to different scenarios not to evolve in a horizontal mismatch.

2.3.2. Wave-current coupling

Wind magnitude and direction being measured at the position 'Leuchtturm Alte Weser' are imposed spatially uniform in the model domain at time intervals of 60 min, both in the FLOW and SWAN module. At intervals of 30 minutes, the spectral wave model SWAN is run in stationary mode to simulate the wave energy propagation and transformation from the open sea model boundary to the shoreline. Wave data (significant wave height Hs, peak wave period Tp, direction and directional spreading) measured at the wave rider buoy 'Elbe' (BSH) are imposed as spatially uniform conditions at the north-western model boundary at intervals of 30 min. This time interval coincides with the sequential two-way-coupling between SWAN and the hydrodynamic module that allows exchanging data on curvilinear model grids via a communication file. Wave parameters and the forcing terms associated with the wave radiation stresses computed by SWAN are read by the hydrodynamic module. In turn, bottom changes, water level and depth-integrated current fields generated by the hydrodynamic module during the assigned run-time of 30 min, are used as input to the computation in SWAN. The model loops through these sequential modules until the simulation is accomplished. The interaction of wave forces (radiation stresses), tidal currents and the changing bed- and water levels is thus realized by a fully coupled wave–current simulation.

2.3.3. Boundary conditions

Time series of water levels, salinity and temperature are imposed at the offshore model boundaries and have been provided and made available through a nesting procedure from a larger North Sea model (Kösters and Winter, 2014) generating consistent water level data that were further improved by data assimilation methods using measured water levels of a gauge at Helgoland (Seiß, 2014).

Simulations are run for the months June to November 2012 suggesting to represent mid-term average hydrodynamic conditions. These morphodynamic simulations are compared to the morphological development in response to an extreme storm. In case of this scenario simulation, water levels at the boundary of the Weser model are generated in a nesting procedure that is different from the above-mentioned: A model cascade from the Continental Shelf to the estuarine mouth has been established (Herrling and Winter, 2014) allowing the reproduction of an extreme storm surge event driven by the low pressure cyclone 'Tilo' from Nov. 5th to 11th 2007 with peak water levels of 4.75 meters above mean sea level at the Outer Weser tidal gauge 'Bremerhaven Alter Leuchtturm' on Nov. 9th around noon. Modelled wind and atmospheric pressure fields provided by the German weather service are applied as meteorological forcing of the storm simulation. Daily-mean upstream discharges of the Weser are available from measurements at a gauge near Intschede and imposed at the estuarine upstream model boundary. The long-term median discharge is 245 m³/s but only 163 m³/s in the year 2012. During the storm simulation of one week, upstream discharges range between 440 and 613 m³/s.

2.3.4. Bed layer model and initial sediment grain-size distribution

The sediment transport equation here applied (Van Rijn et al., 2004) differentiates into bedload and suspended transport regimes considering multiple grain-size fractions and a bed layer model. A stratified bed layer model (van der Wegen et al., 2011) is applied to redistribute multiple sediment grain-size fractions in response to the hydrodynamic forcing. The here selected approach incorporates multiple bed layers that discretize the bed stratigraphy. The active transport layer on top is assigned to have a constant thickness (here selected to be 0.4 m) and interacts directly when sediment is eroded or deposited due to the prevailing sediment transport during one time step. Only sediment fractions in this transport layer are available for erosion. The underlayer replenishes the transport layer after erosion with sediment from beneath. A number of bookkeeping underlayers that can be seen as a buffer or reservoir for the transport layer keep track of sediment deposits. The integrated thickness of all underlayers is variable and controls the overall bed elevation. The total of 15 underlayers at 1 m thickness each have been selected to guarantee sufficient sediment availability. The variable sediment composition within the transport layer is used to calculate the arithmetic mean grain-size.

Four sand fractions of 95, 151, 233 and 571 µm were selected to cover the range of non-cohesive grain-sizes typical for the Outer Weser estuary. This selection is based on an analysis and post-processing of spatially

available surface sediment grain-size measurements of the German Bight (Valerius et al., 2015). The original data consist of 12 grain-size classes ranging from <64 µm to >2000 µm with respective mass-fractions per sediment class; spatially distributed on a raster of 250 m side length covering the entire model domain. Mass-fractions of sediment classes between 63 and 125 µm (2 classes), 125 and 177 µm (1 class), 177 and 354 µm (2 classes), 354 and 2000 µm (5 classes) are merged and normalized in order to obtain 4 new grain-size classes.

2.4. Analysis of model output

2.4.1. Bed elevation range

Computed bed levels are recorded at every grid cell in the model domain at daily and hourly intervals for the simulation from June to Nov. 2012 and the storm simulation (Nov. 5th to 11th 2007), respectively. These are organized in two three-dimensional matrices (grid cell m, n at time t) for further analyses, e.g. to derive minimum and maximum values at each grid cell of all times. The difference of these extremes quantifies the computed range of the parameter value over the simulated period: The bed elevation range (BER) is thus the time-integrated envelope of the bed evolution amplitudes. The BER has been previously applied to describe decadal morphodynamic activity based on bathymetric survey data for the German Bight (Kösters and Winter, 2014; Winter, 2011) or based on simulated bed evolutions at the East Frisian Wadden Sea (Herrling and Winter, 2016).

2.4.2. Sediment volume changes for sub- and intertidal areas

Observed and simulated sediment volume changes are calculated for two different control areas. The larger one covers the Outer Weser area from landwards at Bremerhaven to seawards where the main tidal inlet (navigational) channel widens and discharges into deeper waters; lateral borders are either dike lines or elevated tidal flats in the vicinity of tidal divides (covered area, Fig. 6). The other control area covers the approximate tidal basin of the Fedderwarder Priel with tributaries (covered area, Fig. 8).
Sediment volume changes do not consider varying porosities or consolidation of the bed material and are calculated from time-integrated bed level changes multiplied with the respective grid cell area. Spatially integrated sediment volume that is eroded or deposited at sub- or intertidal areas, respectively, is evaluated proportionally to the sum of all sediment volumes (absolute values) no matter whether they are eroded or deposited. The excess of sediment volume leaving or entering a control area during the evaluated period is not considered in this budget and needs to be quantified in addition.
The differentiation in between sub- and intertidal areas is realized through intersecting digital elevation models based on observed and simulated morphologies with inclined planes that delineate mean high water levels (MHWL) and mean low water levels (MLWL) spanning across the Outer Weser. MHWLs and MLWLs observed at four tidal gauges between the years 2000 and 2009 (Deutsches Gewässerkundliches Jahrbuch 2009) are used for spatial, linear interpolation. Subtidal (intertidal) areas are below MLWL (in between MLWL and MHWL); control areas at a supratidal level turned out to be spatially unimportant and are neglected in this analysis. Areal ratios between sub- and intertidal domains are approx. 2/3 for the control area covering the Outer Weser and approx. 1/3 for the control area covering the tidal basin of the Fedderwarder Priel.

2.5. Model validation

2.5.1. Validation of simulated hydrodynamics

The period used for the validation of simulated hydrodynamics is determined by the availability of measurements of current velocities and waves from Aug. 20th to Oct.12th 2012. Data were observed by upward looking acoustic Doppler current profiler (ADCP); devices at positions WA1 (currents) and WAW2 (currents and waves) had been operated at water depths of 13 and 16 meters at the Outer Weser, respectively. For this period, predicted time series of current magnitudes are compared to measurements at position WA1 and WAW2 with RMSEs of 0.09 and 0.11 m/s, respectively. Significant wave heights and peak wave periods are validated at position WAW2 with RMSEs of 0.19 m (Hs) and 1.63 sec (Tp).

Observed and simulated water levels are evaluated at eight official gauge positions along the Weser estuary for a period of one month from Aug. 20th to Sept. 20th 2012. At the Outer Weser (study area), RMSEs range between 0.06 m at 'Leuchtturm Alte Weser' (ALW), 0.09 m at 'Robbensuedsteert' (RSS) and 0.11 m at 'Bremerhaven Alter Leuchtturm' (BAL). Upstream of the estuarine mouth, modeled water levels are generally higher than observations but still show good approximations of the tidal phase. Close to the upstream model boundary at 'Weserbruecke Bremen' (WBR), the RMSE yet increases to 0.68 m.
Observed and hindcasted water levels of the storm surge are compared qualitatively and show satisfactorily approximations in tidal amplitude and phase at the tidal gauge 'Bremerhaven Alter Leuchtturm' (BAL). (Fig. 2).

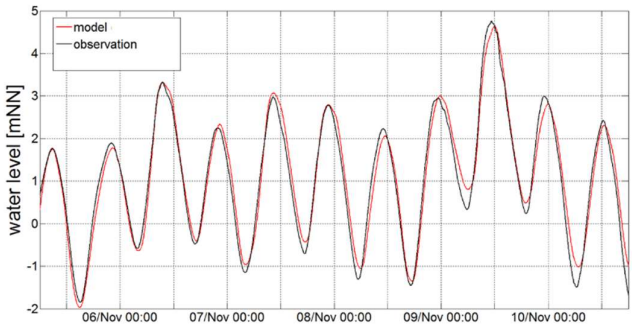

Figure 2. Observed and modelled water levels during the storm event 'Tilo' at the tidal gauge 'Bremerhaven Alter Leuchtturm' (BHV).

2.5.2. Validation of simulated morphodynamics
Spatially overlapping data of tidal flats surveyed in successive years is generally scarce and does not exist for the considered year 2012. The morphology of the Fedderwarder Priel (FWP), a mid-sized tidal channel in the area of interest (Fig. 3c), is regularly and almost annually surveyed. The morphology of this tributary channel is not directly influenced by maintenance dredging of the navigational channel. Bathymetrical data is available for spring 2011 and spring 2012 allowing to evaluate the morphological evolution for this period. It is noted that this data is not directly comparable with the hindcasted morphodynamics of the period from June to Nov. 2012. Predicted morphological differences are linearly extrapolated to one year to allow for a qualitative comparison with observations. A comprehensive morphological study of the FWP based on measured data between 1998 and 2012 showed that the direction and rate of channel migration reveal overall quasi-linear trends at particular channel bends within the FWP (Benninghoff, 2015). Considering the observed morphological changes between spring 2011 and spring 2012, only qualitative comparisons and evaluations can be drawn and used for the morphodynamic model validation (Fig. 3). In the North, at the confluence with the navigational channel the model shows overall best agreement to measurements. Here, at the western main inlet channel, a migration to the West is reproduced by the model. The large intertidal sand bank in between both northern tidal channels of the FWP experiences a strong accumulation in the model and in nature. At the center of the FWP, at the confluence of the two mentioned inlet channels, the deepening of the bed is generally overestimated by the model.

For two different control areas, we evaluated temporally and spatially integrated volumetric changes of morphologies observed between 2005/2007 and 2008/2009 (i), 2008/2009 and 2012 (ii) as well as for simulated morphological evolutions from June to Nov. 2012 (Fig. 4). We distinguish between erosion and deposition at sub- and intertidal areas, respectively (Sect. 2.4.2).
For the larger control area (Outer Weser) and the first observation period (i), volumetric changes are more than twice as large in subtidal channels (35%) compared to intertidal flats (15%), while erosion is equal to deposition at both areas, respectively. For the second observation period (ii), percentages are in the same order of magnitude but with slightly more erosion at subtidal and similarly more deposition at intertidal areas. Proportional volumes of simulated morphological changes compare well to the observations although sedimentation on the intertidal area is slightly underrepresented compared to the observations.

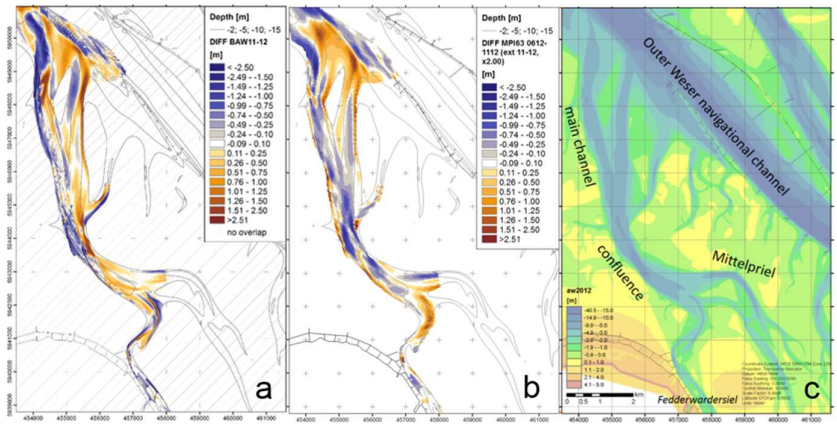

Figure 3. The difference of morphological states, i.e. areas of erosion (blue) and deposition (brown), observed between 2011 and 2012 (a) and of predicted morphological changes between June and Nov. 2012 after a sedimentological and morphological spin-up of approx. 4 months (b). Surveyed morphology of the FWP (c).

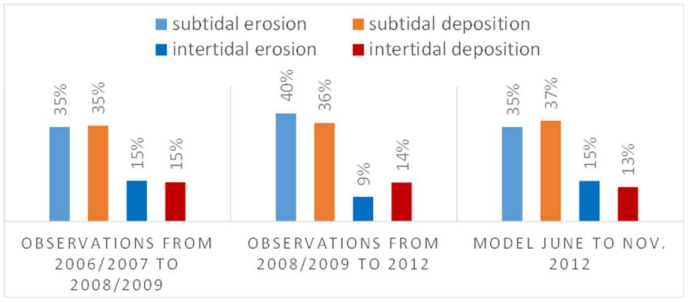

Figure 4. At the Outer Weser estuary, relative morphological changes are evaluated for observed morphologies between 2005/2007 and 2008/2009 (left), 2008/2009 and 2012 (center) and for simulated morphological evolutions from June to Nov. 2012 (right). We differentiate into spatiotemporal integration of erosion or deposition at sub- and intertidal areas; the areal ratio between sub- and intertidal domains is approx. 2/3.

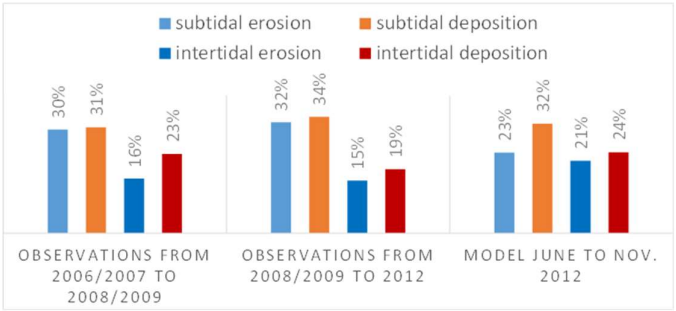

Figure 5. At the tidal basin of the tidal channel Fedderwarder Priel, relative morphological changes are evaluated for observed morphologies between 2005/2007 and 2008/2009 (left), 2008/2009 and 2012 (center) and for simulated morphological evolutions from June to Nov. 2012 (right). We differentiate into spatiotemporal integration of erosion or deposition at sub- and intertidal areas; the areal ratio between sub- and intertidal domains is approx. 1/3.

The smaller control area covers the tidal basin of the Fedderwarder Priel and tributaries (Sect. 2.4.2). Proportional erosion and deposition is consistent for both observation periods and the simulation; in all cases

deposition is higher than erosion at inter- and subtidal areas (Fig. 5). Compared to the observations, the simulated erosive sediment volume is slightly smaller in the subtidal and increased in the intertidal areas. This comparison of spatio-temporal integration of observed and modelled morphological changes for different control volumes and appointed areas delineates variations in between observed changes for different survey periods to be in the same order of magnitude as in between measurements and model. It thus confirms the modelling approach having incorporated the most important physical processes and being a reliable tool to estimate relative morphological changes on spatial scales of tidal basins or tidal basins.

3. Results

3.1. Evaluation of morphological feedbacks in response to distinct hydrodynamic drivers at the Outer Weser area

The bed elevation range (BER) is used to identify and quantify the morphodynamic response to distinct hydrodynamic drivers at the Outer Weser estuary by evaluating (a) tide-induced, (b) wind-induced, (c) wind-wave-induced and (d) sea-wave-induced forcing scenarios. The simulated period is from June to Nov. 2012 and represents average (mostly fair-weather) hydrodynamic conditions. The BER that is assessed with respect to a distinct hydrodynamic driver is expressed proportional to the sum of BERs of all scenarios considered (Fig. 6). For the scenario simulation of only tide-induced forcing, proportionally large BERs of 70 to 100% are identified at tidal channels and shallow subtidal areas (50 to 80%); intertidal areas reveal smaller portions of 0 to 20% with few single peaks of up to 40% (Fig. 6 a).

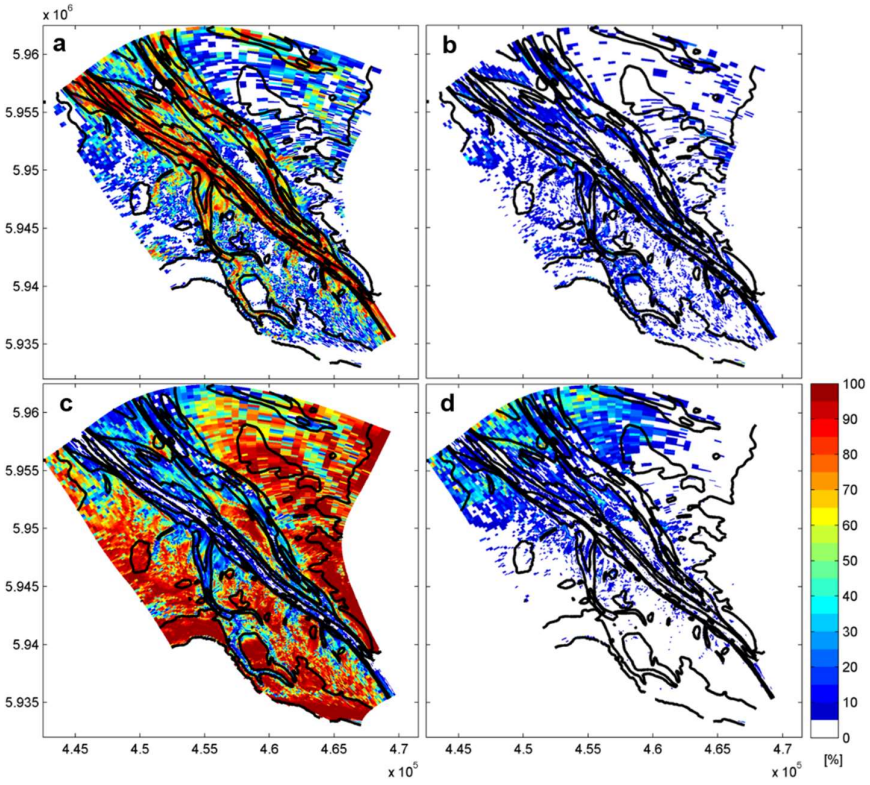

Figure 6: Proportional bed elevation range (BER) to the sum of all BERs of (a) tide-induced, (b) wind-induced, (c) wind-wave-induced and (d) sea-wave-induced forcing scenarios in the Outer Weser estuary evaluated for a simulated period of average hydrodynamic conditions from June to Nov. 2012.

Wind-induced currents, i.e. due to wind shear-stress, have only a small proportional effect on the total morphological activity in the Outer Weser that is quantified to 0 to 20% with few peaks between 20 to 40%. Spatial patterns are less clear to be identified but for the most part tend to concentrate at tidal channels and subtidal areas (Fig. 6 b). Wind-induced waves are generated locally at the Outer Weser model domain. Their proportional effect on the overall morphological feedback reveals a clear spatial pattern in function of the morphological elevation: small portions at tidal channels and subtidal areas (0 to 40%) and increasing portions of 50 to 100% from inter- to supratidal areas (Fig. 6 c). Figure 6 d shows the proportional effect of sea waves being imposed at the seaward model boundary on the total BER. Wave energy that propagates into the Outer Weser model domain is rapidly dissipated on depth-limiting tidal flats and shoals. The relative morphological response to wave-induced sediment stirring and associated morphological activity follows the landward gradient of decreasing wave energy. Proportional BERs are 30 to 60 % at the seaward boundary of the control area and rapidly decrease to 0 to 20% further inside the domain (Fig. 6 d). The large shoal in the north of the FWP is exposed to remaining sea wave energy that only accounts for approx. 10% of the total morphological activity.

Volumetric sediment changes in between the morphology at begin and end of the simulation representing average hydrodynamic conditions are evaluated for the Outer Weser control area (Fig. 7). We subdivided into sub- and intertidal areas; absolute values are integrated in space and time, no matter whether sediments are eroded or deposited (Sect. 2.4.2). Morphological changes as the response to tidal forcing and wind waves show similar portions with 46 and 42%; wind-induced currents and sea waves have much smaller impact on the morphology with only 4 and 8%. Relative portions of wind-induced currents and sea waves do not significantly vary when considering sub- or intertidal areas. The morphological response to tidal forcing and wind-induced waves yet strongly varies in its proportional contribution to the overall morphological feedback depending on the morphological elevation: 57 and 30% for subtidal and 19 and 72% for intertidal areas are evaluated with respect to tidal forcing and wind waves, respectively.

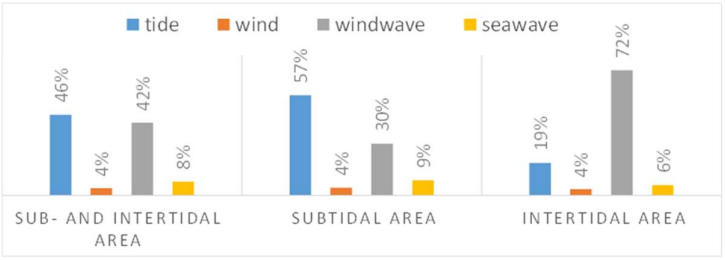

Figure 7. Proportional sediment volume changes for tide-induced, wind-stress-induced, wind-wave-induced and sea-wave-induced forcing scenarios evaluated for a simulated period from June to Nov. 2012 at the Outer Weser control area; differentiation into entire (left), subtidal (center) and intertidal (right) areas.

3.2. Evaluation of morphological feedbacks differentiated in between average and storm hydrodynamic conditions at the Fedderwarder Priel

Spatial patterns of erosion and deposition show the time-integrated morphological evolution for average (mostly fair-weather) and extreme storm conditions at the tidal basin of the tidal channel Fedderwarder Priel (FWP) (Fig. 8 a,b). The morphological response to 6 months of average hydrodynamic forcing is dominated by erosion in the center and northwest and accretion at the large intertidal shoal in the north of the FWP. On intertidal flats, patterns of erosion and deposition alternate with more accretion on higher elevations. For the extreme storm, substantial morphological evolutions are at the tidal channel margins particularly in upwave direction of intertidal shoals. Absolute morphological changes on intertidal flats are small (< 0.03m).
To evaluate morphological changes at margins of intertidal flats, i.e. at the transition between subtidal channels and intertidal shoals, we proposed relevant criteria in order to spatially confine and to investigate whether mid-term deposition during average conditions compensates erosion in response to an extreme storm. The bathymetrical range considered is MLW-2m < depth < MLW+1m and absolute morphological

changes need to be larger than 0.02m in order to be taken into account (Fig. 8c). Spots (red) that satisfy the above-mentioned criteria are identified at the mouth of the FWP tributaries towards the main estuarine tidal inlet, i.e. the navigational channel. In particular at edges of shoals and tidal flats facing the incoming waves, likewise small headlands, these spots characterize areas that are exposed to increased wave-attack. During average hydrodynamic conditions, the model yet predicts increased accumulation of sediments.

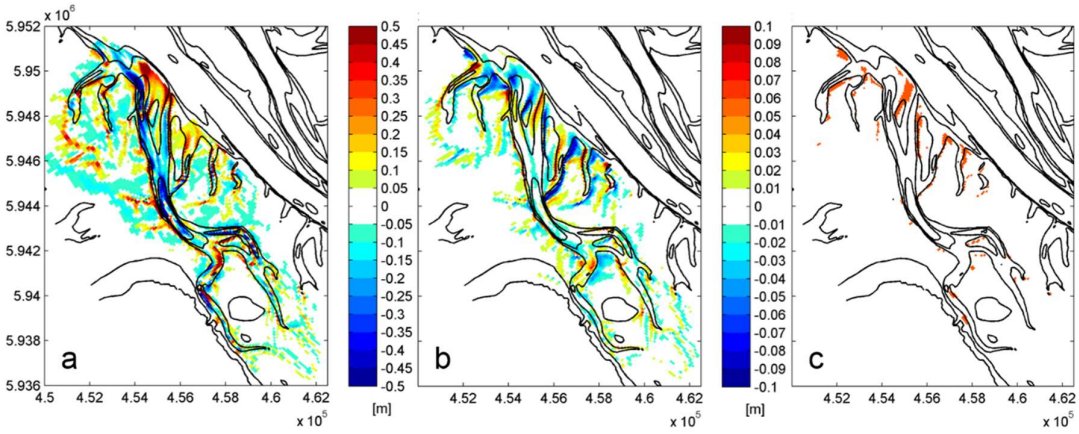

Figure 8. Morphological evolutions at the tidal basin of the Fedderwarder Priel in response to (a) average hydrodynamic conditions, (b) to extreme storm conditions, (c) highlighted areas (red) where erosion in response to storm is compensated by deposition in response to average hydrodynamic conditions.

Relative morphological changes are distinguished at the tidal basin of the FWP. We distinguish morphological changes evaluated for average hydrodynamic conditions of 6 months and the storm event and differentiate in between erosion and deposition at sub- and intertidal domains, respectively (Fig. 9). Considering the forcing of all drivers (currents and waves), relative morphological changes during average hydrodynamic conditions reveal an increased deposition, both at sub- and intertidal areas. For storm conditions, this only holds for subtidal areas whereas at intertidal areas erosion dominates with 35% of total morphological changes. As regards the forcing of currents alone during average conditions, morphological changes are largest at the subtidal where deposition dominates with 42% over erosion 34%; at intertidal areas, deposition (18%) clearly dominates over erosion (7%). Relative morphological changes of the storm in response to currents only are overall well balanced but reveal net deposition on intertidal areas. For the scenario considering waves only, average and storm conditions show similar overall distributions with dominant erosion (both 38%) at intertidal areas.

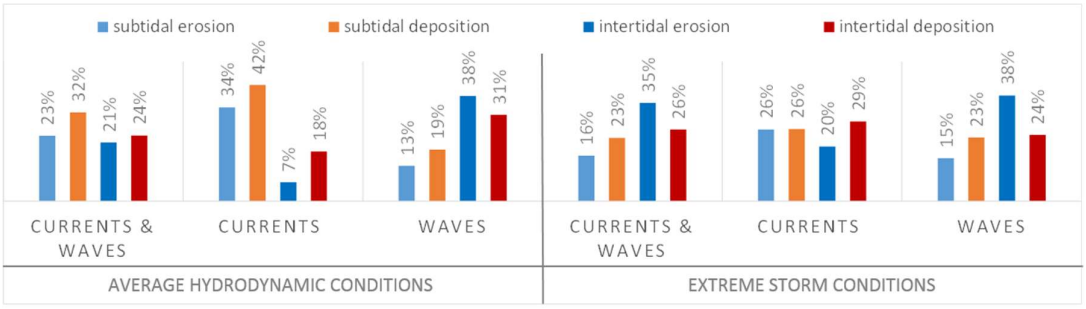

Figure 9. At the tidal basin of the tidal channel Fedderwarder Priel, relative morphological changes are evaluated for average hydrodynamic conditions (left) and extreme storm conditions (right) for different combinations of drivers. We differentiate into spatiotemporal integration of erosion or deposition at sub- and intertidal areas; the areal ratio between sub- and intertidal is approx. 1/3.

4. Discussion

Outside the tidal basin Fedderwarder Priel, the mesh size of the numerical grid is mostly too coarse to adequately resolve smaller tidal channels and tributaries and to reproduce observed morphologies at the scale of single tidal channel cross-sections with good accuracy. We therefore considered larger spatial scales assuming that the overall validity of the morphodynamic model is given when comparing relatively in between different forcing scenarios. Relative morphological changes at defined control areas are evaluated for morphological observations of different survey intervals and periods against model predictions. It is found that variations between different survey periods are in the same order of magnitude as the deviation between measurement and simulation for the equivalent period and control area (Sect. 2.5.2). We thus assume that the model approach and methodology is appropriate to investigate the overall sediment budget and improve our understanding of exchange processes between tidal channels and shoals driven by distinct hydrodynamic drivers.
In contrast to backbarrier tidal basins sheltered by elongated, coast-parallel barrier islands (e.g. East and North Frisian Wadden Sea), the Outer Weser channel-shoal system is likely to be less protected against offshore sea state, particularly during storm conditions. The Outer Weser and other outer estuarine areas can thus be referred to as open-coast intertidal flat systems. Each area is prone to different degrees of wave energy which implies that for each model set-up we need to investigate whether waves need to be taken into account or can be neglected. Model results considering average hydrodynamic conditions, yet indicate that locally wind-generated and fetch-limited waves have a larger mid-term effect on channel-shoal morphodynamics at the Outer Weser than offshore waves propagating into the domain. Offshore-generated waves break and largely dissipate their energy at the depth-limited margin of the outer intertidal flats facing the open North Sea. Morphodynamics at the center of the channel-shoal system, i.e. at the Fedderwarder Priel, are not governed by offshore waves but by locally generated wind-waves (and tides). This is surprising with respect to its more exposed site compared to other Wadden Sea intertidal areas. This let us suppose that at more sheltered back-barrier channel-shoal systems the intensity of tidal flat morphodynamics in response to offshore wave forcing is even less; but the energy of wind-waves may have a comparable intensity as the fetch distance is likely to be similar. Increased bed shear-stress intensity due to wave forcing and thus morphological activity at the Outer Weser tidal flat margins is generally confirmed by the large-scale model study of Kösters and Winter (2014). They investigated the morphological effect of tides, wind and waves, but did not differentiate in between wind- and sea-waves.

5. Conclusions

A process-based morphodynamic model was applied to simulate average hydrodynamic conditions and an extreme storm event at a channel-shoal environment in the Wadden Sea. Relative and absolute morphological changes reveal satisfactory agreements with observations. An analysis of different scenario simulations shows the relative contribution of distinct hydrodynamic drivers, i.e. tides, wind, wind-waves and sea-waves, to the overall morphodynamics. At the Outer Weser channel-shoal system, overall relative morphological changes are governed by tides and locally generated wind waves (46 and 42%). The impact of wind-induced currents and offshore waves is less important (4 and 8%). Morphological changes at subtidal areas, e.g. channel migrations, are largely tide-dominated during fair-weather conditions. Wave-induced sediment stirring, in particular during storms, governs morphological changes at intertidal areas. At the scale of the tidal basin FWP, particular locations are identified that are characterized by erosion as the response to wave-dominant storm conditions; this erosion is compensated by deposition in the course of average tide-dominant (fair-weather) conditions. These areas are located at headland-like edges of intertidal shoals at the mouth of the FWP tributaries discharging into the main inlet channel. This study has a regional focus but may reflect typical characteristics of other open tidal flat environments. The comprehensive methodology is applicable to any other domain where morphodynamic characteristics of channel-shoal systems are evaluated in view of different hydrodynamic drivers.

Acknowledgements

The ongoing research project 'MorphoWeser' is in cooperation with and financed by the German Federal Waterways Engineering and Research Institute (BAW), and through DFG-Research Center/ Cluster of Excellence 'The Ocean in the Earth System', MARUM.

References

Benninghoff, M., 2015. Tidal channel morphodynamics and possible drivers: The example of the Fedderwarder Priel in the Outer Weser estuary. Universität Bremen.

Booij, N., Ris, R.C., Holthuijsen, L.H., 1999. A third-generation wave model for coastal regions 1. Model description and validation. J. Geophys. Res. 104, 7649–7666. doi:10.1029/98JC02622

Deltares, 2014. Delft3D-FLOW, User Manual, Simulation of multi-dimensional hydrodynamic flows and transport phenomena, including sediments. The Netherlands.

Dissanayake, D.M.P.K., Ranasinghe, R., Roelvink, J.A., 2012. The morphological response of large tidal inlet/basin systems to relative sea level rise. Clim. Change 113, 253–276. doi:10.1007/s10584-012-0402-z

Elias, E.P.L., Hansen, J.E., 2013. Understanding processes controlling sediment transports at the mouth of a highly energetic inlet system (San Francisco Bay, CA). Mar. Geol. 345, 207–220. doi:http://dx.doi.org/10.1016/j.margeo.2012.07.003

Friedrichs, C.T., 2011. 3.06-Tidal Flat Morphodynamics: A Synthesis. Treatise Estuar. Coast. Sci. Acad. Press. Waltham 137–170.

Friedrichs, C.T., Aubrey, D.G., 1988. Non-linear tidal distortion in shallow well-mixed estuaries: a synthesis. Estuar. Coast. Shelf Sci. 27, 521–545. doi:http://dx.doi.org/10.1016/0272-7714(88)90082-0

Friedrichs, C.T., Aubrey, D.G., 1996. Uniform bottom shear stress and equilibrium hyposometry of intertidal flats. Mix. estuaries Coast. seas 405–429.

Herrling, G., Winter, C., 2014. Morphological and sedimentological response of a mixed-energy barrier island tidal inlet to storm and fair-weather conditions. Earth Surf. Dyn. 2, 363–382. doi:10.5194/esurf-2-363-2014

Herrling, G., Winter, C., 2016. Spatiotemporal variability of sedimentology and morphology in the East Frisian barrier island system. Geo-Marine Lett. 1–13. doi:10.1007/s00367-016-0462-6

Hofstede, J.L.A., Becherer, J., Burchard, H., 2016. Are Wadden Sea tidal systems with a higher tidal range more resilient against sea level rise? J. Coast. Conserv. 1–8. doi:10.1007/s11852-016-0469-1

Hu, Z., Wang, Z.B., Zitman, T.J., Stive, M.J.F., Bouma, T.J., 2015. Predicting long-term and short-term tidal flat morphodynamics using a dynamic equilibrium theory. J. Geophys. Res. Earth Surf. 120, 1803–1823. doi:10.1002/2015JF003486

Hunt, S., Bryan, K.R., Mullarney, J.C., Pritchard, M., 2016. Observations of asymmetry in contrasting wave- and tidally-dominated environments within a mesotidal basin: implications for estuarine morphological evolution. Earth Surf. Process. Landforms 41, 2207–2222. doi:10.1002/esp.3985

Kösters, F., Winter, C., 2014. Exploring German Bight coastal morphodynamics based on modelled bed shear stress. Geo-Marine Lett. 34, 21–36.

Le Hir, P., Roberts, W., Cazaillet, O., Christie, M., Bassoullet, P., Bacher, C., 2000. Characterization of intertidal flat hydrodynamics. Cont. Shelf Res. 20, 1433–1459. doi:http://dx.doi.org/10.1016/S0278-4343(00)00031-5

Lesser, G.R., Roelvink, J.A., van Kester, J.A.T.M., Stelling, G.S., 2004. Development and validation of a three-dimensional morphological model. Coast. Eng. 51, 883–915. doi:http://dx.doi.org/10.1016/j.coastaleng.2004.07.014

Ris, R.C., Holthuijsen, L.H., Booij, N., 1999. A third-generation wave model for coastal regions 2. Verification. J. Geophys. Res. 104, 7667–7681. doi:10.1029/1998JC900123

Seiß, G., 2014. Erzeugung naturähnlicher Randwerte für den seeseitigen Rand von Ästuarmodellen an der Nordsee. Hamburg.

Valerius, J., Kösters, F., Zeiler, M., 2015. Erfassung von Sandverteilungsmustern zur großräumigen Analyse der Sedimentdynamik auf dem Schelf der Deutschen Bucht. Die Küste 83, 39–63.

van der Wegen, M., Dastgheib, A., Jaffe, B.E., Roelvink, D., 2011. Bed composition generation for morphodynamic modeling: case study of San Pablo Bay in California, USA. Ocean Dyn. 61, 173–186. doi:10.1007/s10236-010-0314-2

van Rijn, L.C., 2007. Unified view of sediment transport by currents and waves. I: Initiation of motion, bed roughness, and bed-load transport. J. Hydraul. Eng. 133, 649–667.

Van Rijn, L.C., Walstra, D.J.R., Van Ormondt, M., 2004. Description of TRANSPOR2004 and implementation in Delft3D-ONLINE. Interim Rep. Prep. DG Rijkswaterstaat, Rijksinst. voor Kust en Zee. Delft Hydraul. Institute, Netherlands.

Winter, C., 2011. Macro scale morphodynamics of the German North Sea coast. J. Coast. Res. 706–710.

Zhou, Z., Coco, G., van der Wegen, M., Gong, Z., Zhang, C., Townend, I., 2015. Modeling sorting dynamics of cohesive and non-cohesive sediments on intertidal flats under the effect of tides and wind waves. Cont. Shelf Res. 104, 76–91. doi:http://dx.doi.org/10.1016/j.csr.2015.05.010